# Dynamic Analysis of Multi-Directional Functionally Graded Panels and Comparative Modeling by ANN

H. Khoshnoodi , M.H. Yas [*], A. Samadinejad

*Department of Mechanical Engineering, Razi University, Kermanshah, Iran*

**ABSTRACT**

In this paper dynamic analysis of multi-directional functionally graded panel is studied using a semi-analytical numerical method entitled the state-space based differential method (SSDQM) and comparative behavior modeling by artificial neural network (ANN) for different parameters. A semi-analytical approach which makes use the three-dimensional elastic theory and assuming the material properties having an exponent-law variation along the axial, radial direction or both directions, the frequency equations of free vibration of multi-directional functionally graded panels are derived. Numerical results are given to demonstrate the convergency and accuracy of the present method. Once the semi-analytical method is validated, an optimal ANN is selected, trained and tested by the obtained numerical results. In addition to the quantitative input parameters is considered as a qualitative input in NN modeling. The results of SSDQM and ANN are compared and the influence of longitude of the panel, material property graded index and circumferential wave number on the non-dimensional natural frequency of functionally graded material (FGM) panels are investigated.                               © 2016 IAU, Arak Branch.All rights reserved.

**Keywords :** Panel; Multi-directional functionally graded; Artificial neural network; Differential quadrature method; State-space method; Dynamic analysis.

## 1 INTRODUCTION

FUNCTIONALLY graded material is a new kind of heterogeneous composite and it possesses continuously varying microstructure and mechanical properties. The advantage of this new kind of material is that no internal boundaries exist and the interfacial stress concentrations can be avoided.

Many studies have been performed to analyze the dynamic behavior of functionally graded structures. Reddy and Cheng[1] presented further development of the linking relationships between vibration frequencies predicted by different theories, and they were extended from a flat plate to a spherical shallow shell. Efraim and Eisenberger [2] presented an exact vibration analysis of variable thickness thick annular isotropic and FGM plates based on the first-order shear deformation theory using finite element method. Nie and Zhong [3] used state-space based differential quadrature to present a semi-analytical solution for three-dimensional vibration of functionally graded circular plates. Dong [4] developed three-dimensional free vibration analysis of functionally graded annular plates using the Chebyshev–Ritz method. Malekzadeh et al. [5] used DQM to study three-dimensional free vibration of thick functionally graded annular plates in thermal environment. Zahedinejad et al.[6] presented A semi-analytical method for three-dimensional free vibration to analysis of functionally graded curved panels. Using the meshless method Free vibration of functionally graded conical shell panels were analyzed by Zhao and Liew [7].

---

[*]Corresponding author.
*E-mail address: yas@razi.ac.ir* (M.H.Yas).

In the above mentioned papers, the material properties are assumed having a smooth variation usually in the axial direction only. However, there are practical occasions which require the materials graded in two or three directions. So, it is necessary to develop appropriate methods to investigate the mechanical responses of multi-directional functionally graded structures. Nemat-Alla [8] investigated reduction of thermal stresses by developing 2D-FGM plate. Nie and Zhong [9] presented dynamic analysis of multi-directional functionally graded annular plates by a semi-analytical numerical method. By using the first-order shear deformation theory and Rayleigh–Ritz procedure, Zhu Su et al. [10] presented a unified solution method for free vibration analysis of functionally graded cylindrical, conical shells and annular plates with general boundary conditions. In this paper, we use a semi-analytical numerical method entitled the state space-based differential quadrature method to study the dynamic behavior of multi-directional functionally graded panels.

On the other hand, the concept of neural networks has been introduced to different branches of engineering [11,12], structural optimization problems [13,14] and functionally graded materials [15,16]. For example Jodaei et al. [17] analyzed free vibration of functionally graded annular plates by semi-analytical numerical method and comparative modeling by ANN. In other paper they [18] studied the free vibration analysis of functionally graded piezoelectric (FGP) annular plates with different boundary conditions by a state-space based differential quadrature method (SSDQM) and compared behavior modeling by an artificial neural network (ANN). Further, it is well known that neural network can be constructed with comparatively simplified procedure for numerical calculations, and the optimum calculation can be carried out without nonlinear and complicated programming methods.

As an alternative and simple modeling technique, ANN was also employed to model the multi-directional FG panels and prediction of different parameters effects on natural frequency of the panels. With this respect, an optimal ANN was selected, trained by training data sets obtained from semi-analytical method with different parameters and also tested by testing data sets. There results obtained were in good agreement with semi-analytical numerical method ones, while keeping the analysis time to a minimum. Finally the results of two methods are illustrated and compared.

## 2    BASIC EQUATIONS
*2.1 Governing equations*

Consider a FGM panel in a cylindrical coordinate system $(r, \theta, z)$, as shown in Fig. 1. where $r, \theta$ and $z$ are in the radial, circumferential and axial directions of the panel.

The equations of elastic equilibrium under the cylindrical coordinate system, in the absence of body forces, are:

$$\frac{\partial \sigma_r}{\partial r} + \frac{1}{r}\frac{\partial \tau_{r\theta}}{\partial \theta} + \frac{\partial \tau_{rz}}{\partial z} + \frac{\sigma_r - \sigma_\theta}{r} = \tilde{\rho}\frac{\partial^2 u_r}{\partial t^2}$$

$$\frac{\partial \tau_{r\theta}}{\partial r} + \frac{1}{r}\frac{\partial \sigma_\theta}{\partial \theta} + \frac{\partial \tau_{\theta z}}{\partial z} + \frac{2\tau_{r\theta}}{r} = \tilde{\rho}\frac{\partial^2 u_\theta}{\partial t^2} \qquad (1)$$

$$\frac{\partial \tau_{rz}}{\partial r} + \frac{1}{r}\frac{\partial \tau_{\theta z}}{\partial \theta} + \frac{\partial \sigma_z}{\partial z} + \frac{\tau_{rz}}{r} = \tilde{\rho}\frac{\partial^2 u_z}{\partial t^2}$$

where $\sigma_r, \sigma_\theta, \sigma_z$ are axial stress componets, $\tau_{rz}$, are shear stress componets, $u_r, u_\theta, u_z$ are displacement componets, $\tilde{\rho}$ denotes material and *t* is time.
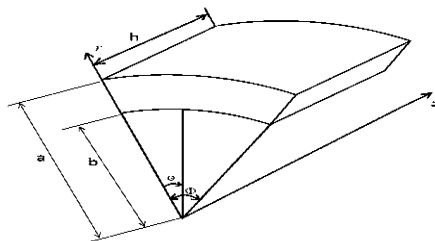


**Fig.1**
A multi-directional functionally graded panel.

The displacement components are related to the strain components through the following relations:

$$\varepsilon_r = \frac{\partial u_r}{\partial r} \quad , \quad \gamma_{\theta z} = \frac{1}{r}\frac{\partial u_z}{\partial \theta} + \frac{\partial u_\theta}{\partial z}$$

$$\varepsilon_\theta = \frac{1}{r}\frac{\partial u_\theta}{\partial \theta} + \frac{u_r}{r} \quad , \quad \gamma_{rz} = \frac{\partial u_r}{\partial z} + \frac{\partial u_z}{\partial r} \tag{2}$$

$$\varepsilon_z = \frac{\partial u_z}{\partial z} \quad , \quad \gamma_{r\theta} = \frac{\partial u_\theta}{\partial r} + \frac{1}{r}\frac{\partial u_r}{\partial \theta} - \frac{u_\theta}{r}$$

The mechanical constitutive relations, which relate the stresses to the strains are as follows:

$$\sigma_r = \tilde{c}_{11}\varepsilon_r + \tilde{c}_{12}\varepsilon_\theta + \tilde{c}_{13}\varepsilon_z \qquad \sigma_\theta = \tilde{c}_{12}\varepsilon_r + \tilde{c}_{22}\varepsilon_\theta + \tilde{c}_{23}\varepsilon_z \qquad \sigma_r = \tilde{c}_{13}\varepsilon_r + \tilde{c}_{23}\varepsilon_\theta + \tilde{c}_{33}\varepsilon_z$$

$$\tau_{\theta z} = \tilde{c}_{44}\gamma_{\theta z} \qquad \tau_{rz} = \tilde{c}_{55}\gamma_{rz} \qquad \tau_{r\theta} = \tilde{c}_{66}\gamma_{r\theta} \tag{3}$$

where $\tilde{c}_{ij}$ are elastic stiffness components.

It is assumed that the material properties have an exponent-law distributions along the axial and radial direction of the panel.

$$\tilde{\rho}(r,z) = \rho^0(0,0)e^{\lambda_1\left(\frac{z}{h}\right)+\lambda_2\left(\frac{r}{a}\right)} \quad , \quad \tilde{c}(r,z) = c^0(0,0)e^{\lambda_1\left(\frac{z}{h}\right)+\lambda_2\left(\frac{r}{a}\right)} \tag{4}$$

where $\rho^0(0,0)$ and $c_{ij}^0(0,0)$ denotes the values of material properties at the center point of the bottom panel, $\lambda_1$ and $\lambda_2$ denote the material property graded indexes in the axial and radial direction, respectively that they can determined by

$$\lambda_1 + \lambda_2 = \ln \tilde{\rho}(a,h) - \ln \rho^0(0,0) = \ln \tilde{c}_{ij}(a,h) - \ln c_{ij}^0(0,0) \tag{5}$$

Considering Eq. (4), the governing equations represented by displacements can be obtained from Eqs. (1)-(3).

$$E.\xi = 0 \tag{6}$$

where $\xi = \begin{bmatrix} u_r & u_\theta & u_z \end{bmatrix}^T$, the expression of the matrix $E$ is given in Appendix A.1.

*2.2 Boundary conditions*

The following simply supported conditions are imposed at the edges of the cylindrical panel:

$$u_r = 0, \ \tau_{rz} = 0, \ \sigma_\theta = 0 \qquad \theta = 0, \Phi \tag{7}$$

For free vibration problems, boundary conditions at the top and bottom surfaces are assumed as the following.

$$at \ z = 0 \ and \ h : \tau_{rz} = 0, \tau_{\theta z} = 0, \sigma_z = 0 \tag{8}$$

## 3   SEMI-ANALYTICAL SOLUTION

State-space based differential quadrature method is a combination of the state-space method and differential quadrature method. The analytical solution in the axial direction can be acquired using the state-space method and approximate solution in the radial direction can be obtained using differential quadrature method.

The following assumed solutions satisfy the simply supported opposite edges at $\theta = 0, \phi$:

$$u_r\left(r,\theta,z,t\right)=\sum_{m=1}^{\infty}\tilde{u}_r\left(r,z\right)\sin\left(\beta_m\theta\right)e^{i\omega t}$$

$$u_\theta\left(r,\theta,z,t\right)=\sum_{m=1}^{\infty}\tilde{u}_\theta\left(r,z\right)\cos\left(\beta_m\theta\right)e^{i\omega t} \quad , \quad \beta_m=\frac{m\pi}{\varnothing} \quad \left(m=1,2,\ldots\right) \tag{9}$$

$$u_z\left(r,\theta,z,t\right)=\sum_{m=1}^{\infty}\tilde{u}_z\left(r,z\right)\sin\left(\beta_m\theta\right)e^{i\omega t}$$

where $i=\sqrt{-1}$, "$m$" is the circumferential wave numbers and $\omega$ is the natural angular frequency of the vibration. using the following non-dimensional parameters,

$$Z=\frac{z}{h} \;,\; R=\frac{r}{a} \;,\; U_R=\frac{\tilde{u}_r}{h} \;,\; U_\theta=\frac{\tilde{u}_\theta}{h} \;,\; U_z=\frac{\tilde{u}_z}{h} \;,\; \bar{c}_{ij}^{\,0}=\frac{c_{ij}^{\,0}}{c_{11}^{\,0}} \;,\; \Omega=\omega h\sqrt{\frac{\rho^0}{c_{11}^{\,0}}} \tag{10}$$

By combining Eq. (6) and employing Eqs. (9) and (10) and using state-space:

$$\frac{\partial}{\partial Z}\begin{bmatrix}\xi\\\zeta\end{bmatrix}=\begin{bmatrix}0 & I\\M_1(R) & M_2(R)\end{bmatrix}\begin{bmatrix}\xi\\\zeta\end{bmatrix} \;,\; \left(i=1,2,\ldots,N\right) \tag{11}$$

where $\xi=\begin{bmatrix}U_R & U_\theta & U_Z\end{bmatrix}^T$, $\zeta=\begin{bmatrix}\dfrac{\partial U_R}{\partial Z} & \dfrac{\partial U_\theta}{\partial Z} & \dfrac{\partial U_Z}{\partial Z}\end{bmatrix}^T$. $I$ is the unity matrix of $3\times3$ matrices $M_1(R)$ and $M_2(R)$ are the functions of the variable $R$ and the expressions in Appendix (A.2).

A semi-analytical procedure with the aid of DQM technique was recently developed by Chen and Bian [19]. In this method the nth order partial derivative of a continuous function $f(r,z)$ with respect to $r$ at a given point $r_i$ can be approximated as a linear sum of weighted function values at all of the discrete points in the domain of $r$, i.e.

$$\frac{\partial^2 f\left(r_i\right)}{\partial r^2}=\sum_{k=1}^{N}w_{ik}^{(n)}f\left(r_k\right) \qquad i=1,\ldots,N \qquad n=1,\ldots,N-1 \tag{12}$$

where $N$ is the number of sampling points, and $w_{ik}^{(n)}$ are the $r_i$ dependent weight coefficients [19,20]. In order to determine the weighting coefficients $w_{ik}^{(n)}$, the Lagrange interpolation basic functions are used, as the test functions and explicit formulas for computing these weighting coefficients can be obtained as [21]:

$$w_{ij}^{(1)}=\frac{M^{(1)}\left(r_i\right)}{\left(r_i-r_j\right)M^{(1)}\left(r_i\right)} \qquad i,j=1,2,\ldots,N,i\neq j \tag{13}$$

where

$$M^{(1)}\left(r_i\right)=\prod_{j=1,i\neq j}^{N}\left(r_i-r_j\right) \tag{14}$$

For first-order derivative, i.e. $n=1$, and for higher-order derivatives, one can use the following relations iteratively:

$$w_{ij}^{(n)}=n\left(w_{ii}^{(n-1)}w_{ij}^{(1)}-\frac{w_{ij}^{(n-1)}}{\left(r_i-r_j\right)}\right) \qquad i,j=1,2,\ldots,N,i\neq j,n=2,3,\ldots,N-1 \tag{15}$$

$$w_{ii}^{(n)}=-\sum_{j=1,i\neq j}^{N}w_{ij}^{(n)} \qquad i=1,2,\ldots,N \;,\; n=1,2,\ldots,N-1$$

A simple and natural choice of the grid distribution is the uniform grid spacing rule. However, it was found that non- uniform grid spacing yields results with better accuracy [22]. Hence, in this work, the Chebyshev–Gauss–Lobatto quadrature points are used, i.e. [21]:

$$r_i = \frac{1}{2}\left(1 - \cos\left(\frac{i-1}{N-1}\pi\right)\right), \qquad i = 1,2,\ldots,N \tag{16}$$

Using DQM:

$$\frac{\partial}{\partial Z}\begin{bmatrix} \tilde{\xi}_i \\ \tilde{\zeta}_i \end{bmatrix} = \begin{bmatrix} 0 & I \\ M_1'(R_i) & M_2'(R_i) \end{bmatrix}\begin{bmatrix} \tilde{\xi}_i \\ \tilde{\zeta}_i \end{bmatrix} \tag{17}$$

The solution to Eq. (17) can be written as [23]:

$$\begin{bmatrix} \tilde{\xi}_i(Z) \\ \tilde{\zeta}_i(Z) \end{bmatrix} = exp\left(B_i.Z\right)\begin{bmatrix} \tilde{\xi}_i(0) \\ \tilde{\zeta}_i(0) \end{bmatrix}, \qquad i = 1,2,\ldots,N \tag{18}$$

where:

$$B_i = \begin{bmatrix} 0 & I \\ M_1'(R_i) & M_2'(R_i) \end{bmatrix} \tag{19}$$

where, $exp\left(B_i.Z\right)$ is the matrix exponential function. $\tilde{\xi}_i(Z), \tilde{\zeta}_i(Z), \tilde{\xi}_i(0)$ and $\tilde{\zeta}_i(0)$ are the values of the state variables at arbitrary plane $Z$ and the bottom plane $Z = 0$, respectively. From Eq. (18), we get:

$$\begin{bmatrix} \tilde{\xi}_i(1) \\ \tilde{\zeta}_i(1) \end{bmatrix} = expB_i\begin{bmatrix} \tilde{\xi}_i(0) \\ \tilde{\zeta}_i(0) \end{bmatrix}, \qquad (i = 1,2,\ldots,N) \tag{20}$$

where $\tilde{\xi}_i(1)$ and $\tilde{\zeta}_i(1)$ are the values of the state variables at the top plane $Z = 1$. By applying boundary conditions of bottom and top surfaces of the panel the following equations can be found:

$$\begin{bmatrix} \tilde{\zeta}_i(0) \\ \tilde{\zeta}_i(1) \end{bmatrix} = D.\begin{bmatrix} \tilde{\xi}_i(0) \\ \tilde{\xi}_i(1) \end{bmatrix}, \qquad (i = 1,2,\ldots,N) \tag{21}$$

where $D$ is the $(6N \times 6N)$ matrix and its expression is omitted. Then, substituting Eq. (21) into Eq. (20) and eliminating the first derivatives of the displacements $\tilde{\zeta}_i(0)$ and $\tilde{\zeta}_i(1)$, we get:

$$B.\begin{bmatrix} \tilde{\xi}_i(0) \\ \tilde{\xi}_i(1) \end{bmatrix} = 0 , \qquad (i = 1,2,\ldots,N) \tag{22}$$

where $B$ denotes the $(6N \times 6N)$ matrix. The boundary conditions on the circumferential edges, shown in Eq. (7), can also be written as the discretized forms. And substituting the circumferential boundary conditions into Eq. (24), we get a non-trivial solution by setting.

$$\det B = 0 \tag{23}$$

The above equation is solved to obtain a set of frequencies of multi-dimensional functionally graded panels. The

corresponding mode shape can be determined from Eq. (22).

**Table 1**
Convergence results of the first three non-dimensional frequencies for FG panel ($a = 1m, b = 0.2m, h = 0.1m, \phi = 2\pi$).

| Graded indexes | Frequencies | Number of points along the radial direction while using DQM | | | | Ref. [10] |
|---|---|---|---|---|---|---|
| | | 5 | 7 | 9 | 10 | |
| $\lambda_1 = 1$ | $\Omega_1$ | 0.0776 | 0.0796 | 0.0805 | 0.0807 | 0.0807 |
| $\lambda_2 = 0$ | $\Omega_2$ | 0.0811 | 0.0815 | 0.0816 | 0.0817 | 0.0837 |
| | $\Omega_3$ | 0.0967 | 0.0958 | 0.0965 | 0.095 | 0.0961 |
| $\lambda_1 = 0$ | $\Omega_1$ | 0.0825 | 0.082 | 0.0816 | 0.0817 | 0.0835 |
| $\lambda_2 = 1$ | $\Omega_2$ | 0.0876 | 0.0869 | 0.0868 | 0.0866 | 0.087 |
| | $\Omega_3$ | 0.1041 | 0.1025 | 0.1016 | 0.1011 | 0.1006 |
| $\lambda_1 = 1$ | $\Omega_1$ | 0.0829 | 0.0825 | 0.0824 | 0.0822 | 0.0817 |
| $\lambda_2 = 1$ | $\Omega_2$ | 0.0877 | 0.087 | 0.0867 | 0.0868 | 0.0851 |
| | $\Omega_3$ | 0.1047 | 0.1037 | 0.1037 | 0.1032 | 0.0985 |

**Table 2**
Analysis results of the lowest three non-dimensional frequencies for different angle and circumferential wave number ($a = 1m, b = 0.8m, h = 0.1m, \lambda_1 = \lambda_2 = 1$).

| Angle of FG panel | m=1 | | | m=2 | | | m=3 | | |
|---|---|---|---|---|---|---|---|---|---|
| | $\Omega_1$ | $\Omega_2$ | $\Omega_3$ | $\Omega_1$ | $\Omega_2$ | $\Omega_3$ | $\Omega_1$ | $\Omega_2$ | $\Omega_3$ |
| $\pi/6$ | 0.3928 | 0.3975 | 0.4064 | 0.7903 | 0.7998 | 0.818 | 1.1844 | 1.1988 | 1.2265 |
| $\pi/4$ | 0.2537 | 0.2565 | 0.2617 | 0.5262 | 0.5325 | 0.5445 | 0.7903 | 0.7998 | 0.818 |
| $\pi/3$ | 0.1695 | 0.1707 | 0.173 | 0.3928 | 0.3975 | 0.4064 | 0.5924 | 0.5995 | 0.6131 |
| $\pi/2$ | 0.1679 | 0.1699 | 0.1737 | 0.2537 | 0.2565 | 0.2617 | 0.3928 | 0.3975 | 0.4064 |
| $2\pi/3$ | 0.1329 | 0.1346 | 0.1377 | 0.1695 | 0.1707 | 0.173 | 0.29 | 0.2933 | 0.2995 |
| $\pi$ | 0.1036 | 0.1049 | 0.1075 | 0.1679 | 0.1699 | 0.1733 | 0.1695 | 0.1707 | 0.173 |
| $4\pi/3$ | 0.0916 | 0.0928 | 0.0951 | 0.134 | 0.1346 | 0.1377 | 0.1876 | 0.1897 | 0.1938 |
| $3\pi/2$ | 0.0882 | 0.0893 | 0.0915 | 0.1225 | 0.124 | 0.127 | 0.1679 | 0.1699 | 0.1737 |

**Table 3**
Analysis results of the lowest three non-dimensional frequencies for different parameters and ratio of material property graded indexes ($h/a = 0.1, m = 1, \phi = 2\pi/3$).

| b/a | $\lambda_2/\lambda_1 = 1$ | | | $\lambda_2/\lambda_1 = 1.5$ | | | $\lambda_2/\lambda_1 = 2$ | | | $\lambda_2/\lambda_1 = 2.5$ | | |
|---|---|---|---|---|---|---|---|---|---|---|---|---|
| | $\Omega 1$ | $\Omega 2$ | $\Omega 3$ | $\Omega 1$ | $\Omega 2$ | $\Omega 3$ | $\Omega 1$ | $\Omega 2$ | $\Omega 3$ | $\Omega 1$ | $\Omega 2$ | $\Omega 3$ |
| 0.8 | 0.1329 | 0.1346 | 0.1377 | 0.1288 | 0.1305 | 0.1338 | 0.1229 | 0.1247 | 0.1281 | 0.1136 | 0.1158 | 0.1197 |
| 0.82 | 0.1329 | 0.1344 | 0.1372 | 0.1288 | 0.1303 | 0.1332 | 0.1228 | 0.1244 | 0.1275 | 0.1136 | 0.1155 | 0.1191 |
| 0.84 | 0.1329 | 0.1342 | 0.1367 | 0.1288 | 0.1301 | 0.1327 | 0.1228 | 0.1242 | 0.127 | 0.1135 | 0.1152 | 0.1184 |
| 0.86 | 0.1328 | 0.134 | 0.1361 | 0.1287 | 0.1299 | 0.1321 | 0.1227 | 0.124 | 0.1264 | 0.1135 | 0.115 | 0.1177 |
| 0.88 | 0.1328 | 0.1338 | 0.1356 | 0.1287 | 0.1297 | 0.1316 | 0.1227 | 0.1238 | 0.1258 | 0.1134 | 0.1147 | 0.1171 |
| 0.9 | 0.1328 | 0.1336 | 0.1351 | 0.1287 | 0.1295 | 0.1311 | 0.1227 | 0.1236 | 0.1252 | 0.1134 | 0.1144 | 0.1164 |
| 0.92 | 0.1327 | 0.1334 | 0.1346 | 0.1286 | 0.1293 | 0.1305 | 0.1226 | 0.1233 | 0.1247 | 0.1134 | 0.1142 | 0.1157 |
| 0.94 | 0.1327 | 0.1332 | 0.1341 | 0.1286 | 0.1291 | 0.13 | 0.1226 | 0.1231 | 0.1241 | 0.1133 | 0.1139 | 0.1151 |

## 4 NEURAL NETWORK MODELING
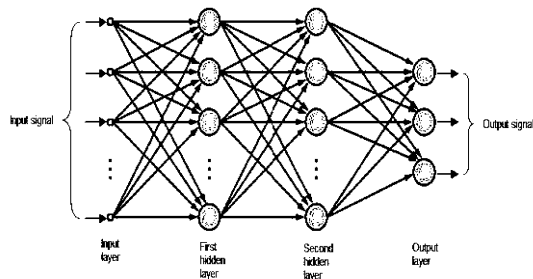


**Fig.2**
Schematic diagram of ANN model.

*4.1 Overview of NNs*

Artificial Neural Networks (NNs) are computer models that mimic the biological nervous system. An NN can be defined as a massively parallel distribute processor that has a natural propensity for storing experiential knowledge and making it available for use [24]. The main component of this model is the structure of its information processing unit. A biological neuron is made up of four main parts: dendrites, synapses, axon and the cell body. The basic element of an NN is the artificial neuron which consists of three main components namely as weights, bias, and an activation function. Each neuron receives inputs $x_1 : x_2 : .... : x_n$, attached with a weight $w_i$ which shows the connection strength for that input for each connection. Each input is then multiplied by the corresponding weight of the neuron connection. A bias $b_i$ can be defined as a type of connection weight with a constant nonzero value added to the summation of inputs and corresponding weights $u$, given by:

$$u_i = \sum_{i=1}^{N} w_{i_j} x_j + b_i$$  (24)

The summation $u_i$ is transformed using a scalar-to-scalar function called an ''activation or transfer function,'' $f(u_i)$ yielding a value called the unit's ''activation,'' given by:

$$Y_i = f(u_i)$$  (25)

Activation functions serve to introduce nonlinearity into NNs which makes NNs so powerful. NNs are commonly classified by their network topology (i.e. feed back, feed forward) and learning or training algorithms (i.e. supervised, unsupervised). For example, a multilayer feed forward NN with back propagation indicates the architecture and learning algorithm of the NN.

*4.2 Optimal NN model selection*
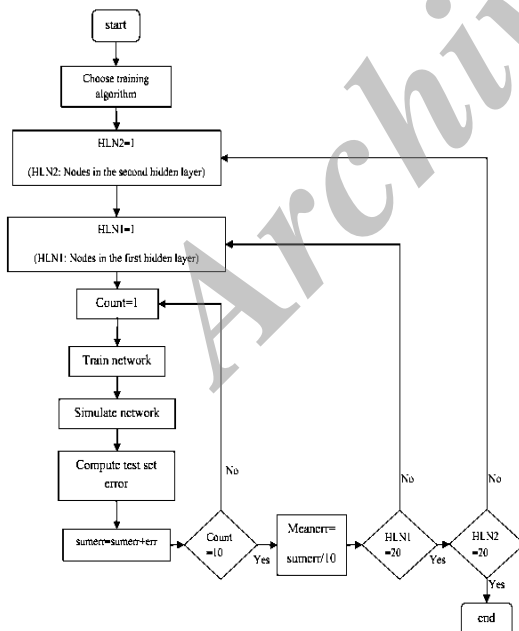


**Fig.3**
Flowchart of optimal NN selection.
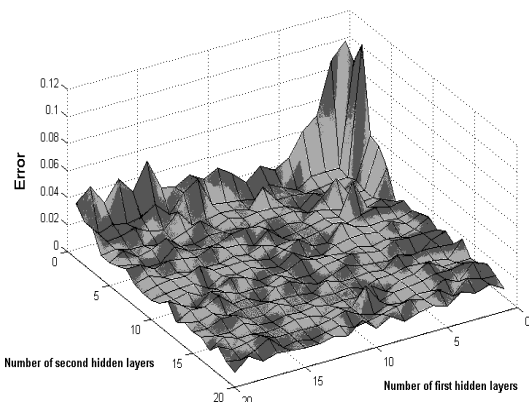
**Fig.4**
Errors of NN architectures with different neurons in hidden layers.

The performance of an NN model mainly depends on the network architecture and parameter settings. The neuron model and the architecture of a neural network describe how a network transforms its input into an output. This transformation can be viewed as a computation. One of the most difficult tasks in NN studies is to find this optimal network architecture. There are many heuristic techniques described in the neural network literature to perform various tasks within the supervised learning paradigm, such as optimizing training, selecting an appropriately sized network, and predicting how much data will be required to achieve a particular generalization performance. In this study Matlab NN toolbox is used for NN applications. Matlab NN toolbox randomly assigns the initial weights for each run each time which considerably changes the performance of the trained NN even all parameters and NN architecture are kept constant. This leads to extra difficulties in the selection of optimal network architecture and parameter settings.

To overcome this difficulty a program has been developed in Matlab which handles the trial and error process automatically. The program tries various number of layers and neurons (less than20) in the hidden layers both for first and second hidden layers for a constant validation check for several times and record the mean of MAE (mean absolute %error) or MSE (mean squared error) of the testing set, as the training of the testing set is more critical. All of the errors for different networks are stored and compared to select the best network. This process is repeated $N$ times, where $N$ denotes the number of hidden nodes for the first hidden layer. This whole process is repeated for changing number of nodes in the second hidden layer.

More over this selection process is performed for different back propagation training algorithms such as trainlm, trainscg and trainbfg, which the best one here selected as trainlm which is Levenberg–Marquardt algorithm. Levenberg–Marquardt (LM) algorithm randomly divides put vectors and target vectors into three sets including training, validation and testing. Changing the relative percentages of these three sets could slightly improve the generalization process. In this study, 60% of whole data is specified as the training data in which the network would be adjusted according to its error. Similarly 20% of database is considered as the validating data which is used to measure network generalization and to halt training when generalization stop improving. Finally the remaining 20% of whole data is specified as the testing data which has no effect on training and so provide san independent measure of network performance during and after training. In this program up to 20 neurons in each hidden layer is tested and the optimal network is selected based on the minimum MAE. The optimal NN architecture was obtained as 8-14-18-3 (Fig. 2. Schematic diagram of 8-n-m-3 ANN model).
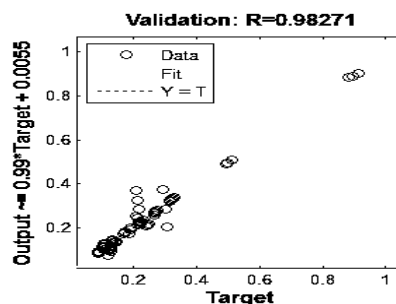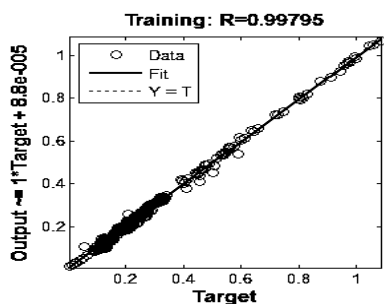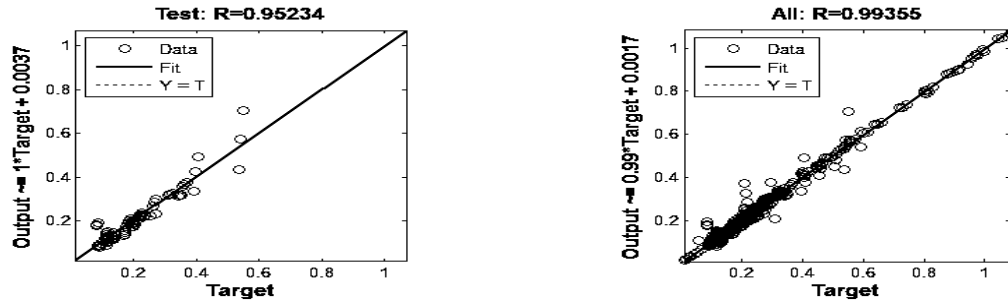
**Fig.5**
Regressions of training, validation and test data simulated by NN .

**Table 4**
Comparison study of lowest three frequencies of functionally graded panel using SSDQM and ANN ($a=1m, b=0.8m, \phi=\pi/3, \lambda_1=\lambda_2=1$).

| h (m) | Method | m= 0 | | | m= 1 | | | m= 2 | | |
|-------|--------|------|------|------|------|------|------|------|------|------|
| | | $\Omega 1$ | $\Omega 2$ | $\Omega 3$ | $\Omega 1$ | $\Omega 2$ | $\Omega 3$ | $\Omega 1$ | $\Omega 2$ | $\Omega 3$ |
| 0.12 | SSDQM | 0.104 | 0.1056 | 0.1096 | 0.2213 | 0.2235 | 0.2277 | 0.474 | 0.4797 | 0.4905 |
| | ANN | 0.1064 | 0.1222 | 0.1134 | 0.2213 | 0.2293 | 0.2347 | 0.4601 | 0.4772 | 0.4851 |
| 0.14 | SSDQM | 0.1212 | 0.1232 | 0.1279 | 0.2679 | 0.2708 | 0.2764 | 0.5555 | 0.5622 | 0.575 |
| | ANN | 0.1199 | 0.1333 | 0.1303 | 0.272 | 0.2803 | 0.2865 | 0.5525 | 0.5655 | 0.5767 |
| 0.16 | SSDQM | 0.1383 | 0.141 | 0.1462 | 0.3128 | 0.3164 | 0.3233 | 0.6373 | 0.645 | 0.6597 |
| | ANN | 0.1413 | 0.1477 | 0.1492 | 0.3211 | 0.32655 | 0.3322 | 0.6441 | 0.6531 | 0.6703 |
| 0.18 | SSDQM | 0.1555 | 0.1588 | 0.1644 | 0.3574 | 0.3616 | 0.3698 | 0.7194 | 0.7281 | 0.7447 |
| | ANN | 0.1645 | 0.1645 | 0.168 | 0.3661 | 0.3691 | 0.3748 | 0.728 | 0.7358 | 0.7598 |
| 0.2 | SSDQM | 0.1728 | 0.1768 | 0.1827 | 0.402 | 0.4069 | 0.4162 | 0.8014 | 0.8111 | 0.8296 |
| | ANN | 0.1824 | 0.1810 | 0.1850 | 0.4068 | 0.4104 | 0.4176 | 0.8062 | 0.8153 | 0.8437 |
| 0.22 | SSDQM | 0.1857 | 0.1894 | 0.191 | 0.4468 | 0.4523 | 0.4627 | 0.8834 | 0.8941 | 0.9145 |
| | ANN | 0.1946 | 0.1947 | 0.1993 | 0.4461 | 0.4527 | 0.4614 | 0.8852 | 0.8963 | 0.9250 |
| 0.24 | SSDQM | 0.2 | 0.2066 | 0.2087 | 0.4918 | 0.4979 | 0.5095 | 0.9651 | 0.9768 | 0.9991 |
| | ANN | 0.2043 | 0.2072 | 0.2122 | 0.4871 | 0.498 | 0.5067 | 0.9659 | 0.9800 | 1.0054 |
| 0.26 | SSDQM | 0.2148 | 0.2236 | 0.2262 | 0.537 | 0.5436 | 0.5563 | 1.0466 | 1.0592 | 1.0835 |
| | ANN | 0.2155 | 0.2229 | 0.2273 | 0.5313 | 0.5489 | 0.5553 | 1.045 | 1.0632 | 1.0822 |

## 5  RESULTS AND DISCUSSION

The material properties of the panel are assumed as the exponent-law variation in the axial and radial direction shown in Eq. (4). The Young's modulus in $r=0$ and $z=0$ is $E=380\,GPa$ and Poisson's ratio is chosen as constant, $\upsilon=0.3$. The material density at the center of the bottom plane is $\rho=3800\,kg/m^3$. The equally spaced discrete points are adopted while using the differential quadrature method. In the following we will verify the presented solutions and investigate the dynamic behavior of multi-directional functionally graded panel under different conditions.

As a first, the convergence behavior and accuracy of the semi-analytical numerical method for the first three frequency parameters of FG panels of different material property graded indexes are studied in Table 1. The results are compared with those of the three-dimensional elasticity solutions of Nie and Zhong [9], which were obtained using the semi-analytical numerical method for multi-directional FG annular plates. The results for FG panels with different angles and circumferential wave numbers are presented in Table 2. and for different parameters and ratio of material property graded indexes FG panels are given in Table 3. In this table, it is observed that the non-dimensional frequencies decreases through the decrease of thickness for $a=0.1$, but with increase in the parameter $b$, this frequency decreases slowly.

As another method (ANN), the database in this study included 190 data sets for different parameters obtained from SSDQM analysis. Again 52 data sets with different incremental values of input parameters are prepared so that the NN to be tested again with new sets of data. After the network memorizes the training set (at the expense of

generalizing more poorly), training is stopped. This technique automatically avoids the problem of over-fitting, which plagues many optimization and learning algorithms. The flowchart of the whole process is shown in Fig. 3 and the errors are shown in Fig. 4. in which the minimum error point is highlighted.

Fig. 5 shows the regression of network. If there were a perfect fit (outputs exactly equal to targets), the regression would be 1, and the y-intercept would be 0. In this study, the output tracks the targets very well for training, testing, and validation, and the R-value is over 0.95 for the total response.

In order to investigate the influence of different parameters on non-dimensional frequency, the results of semi-analytical solution and ANN model are comparatively illustrated in the following table and figures. You can see that the numbers are close in Table 4. for lowest three non-dimensional frequencies for different longitude and circumferential wave numbers. it is noted that increase of circumferential wave number leads to increase in the natural frequency. It also shows that increase frequencies with increase of longitude.

The variations of lowest three natural frequencies for different longitude against ratio of material property gradient index are depicted in Figs. 6-8. It can be seen obviously that for both SSDQM and ANN results, the natural frequency increase with the increase of material property gradient index in radial direction.
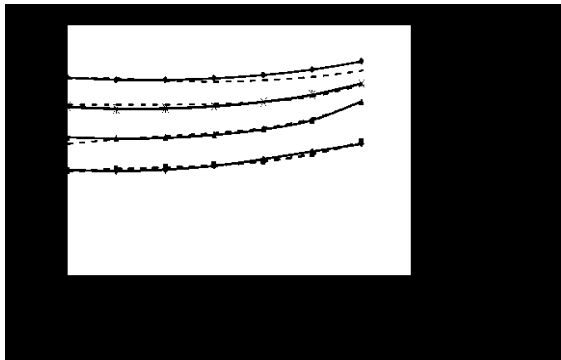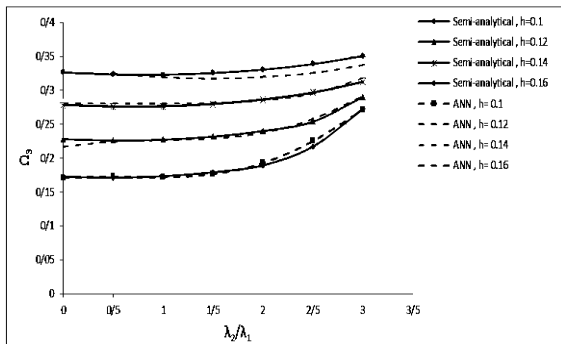


**Fig.6**
Variation of the first non-dimensional frequency vs. ratio of gradient indexes at different longitude ($a=1m, b=0.8m, m=1$).
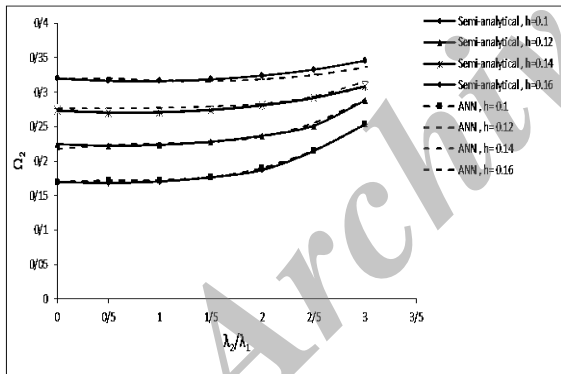


**Fig.7**
Variation of the second non-dimensional frequency vs. ratio of gradient indexes at different longitude ($a=1m, b=0.8m, m=1$).



**Fig.8**
Variation of the third non-dimensional frequency vs. ratio of gradient indexes at different longitude ($a=1m, b=0.8m, m=1$).

## 6   CONCLUSIONS

Based on the three-dimensional elastic theory and assuming the mechanical properties having an exponent-law variation along the axial, radial direction or both directions, the dynamic behavior of multi-directional functionally graded panels is studied using a semi-analytical numerical method entitled the state space-based differential quadrature method. The convergence and accuracy of the present method is validated by comparing the obtained results with those published in the literature. Then, an optimal ANN is selected, trained and tested by the numerical results obtained by SSDQM.

Finally a comparative parametric study of the results obtained by SSDQM and ANN are presented in which the influences of longitude of the panel, material property graded index and circumferential wave number on the non-dimensional natural frequency of FGM panels. The results show that ANN can acceptably model the behavior of functionally graded panels with different parameters. The conclusions that can be made from the parametric study are as following:

- An optimal ANN can be obtained to predict the natural frequencies rather precisely for different parameters without keeping the calculation time.
- ANN model can acceptably predict and show all the trends which agree well with semi-analytical trends.
- The non-dimensional natural frequencies of the functionally graded panels decrease slowly with the decrease of the thickness.
- Increase of angle of panel leads to decrease in the natural frequency.
- For both SSDQM and ANN results, the natural frequency increases with the increase of material property gradient index, longitude and circumferential wave number.

## APPENDIX A

$$E = \begin{bmatrix} E_{11} & E_{12} & E_{13} \\ E_{21} & E_{22} & E_{23} \\ E_{31} & E_{32} & E_{33} \end{bmatrix}$$

$$E_{11} = c_{11}^0 \left( \frac{1}{r}\frac{\partial}{\partial r} + \frac{\partial^2}{\partial r^2} + \frac{\lambda_2}{a}\frac{\partial}{\partial r} \right) + c_{12}^0 \frac{\lambda_2}{a}\frac{1}{r} - c_{22}^0 \frac{1}{r^2} + c_{55}^0 \left( \frac{\partial^2}{\partial z^2} + \frac{\lambda_1}{h}\frac{\partial}{\partial z} \right) + c_{66}^0 \frac{1}{r^2}\frac{\partial^2}{\partial \theta^2} - \rho^0 \frac{\partial^2}{\partial t^2}$$

$$E_{12} = c_{12}^0 \left( \frac{1}{r}\frac{\partial^2}{\partial r \partial \theta} + \frac{\lambda_2}{a}\frac{1}{r}\frac{\partial}{\partial \theta} \right) - c_{22}^0 \frac{1}{r^2}\frac{\partial}{\partial \theta} + c_{66}^0 \left( \frac{1}{r}\frac{\partial^2}{\partial r \partial \theta} - \frac{1}{r^2}\frac{\partial}{\partial \theta} \right)$$

$$E_{13} = c_{13}^0 \left( \frac{\partial^2}{\partial r \partial z} + \frac{1}{r}\frac{\partial}{\partial z} + \frac{\lambda_2}{a}\frac{\partial}{\partial z} \right) - c_{23}^0 \frac{1}{r}\frac{\partial}{\partial z} + c_{55}^0 \left( \frac{\partial^2}{\partial r \partial z} + \frac{\lambda_1}{h}\frac{\partial}{\partial r} \right)$$

$$E_{21} = c_{12}^0 \left( \frac{1}{r}\frac{\partial^2}{\partial r \partial \theta} \right) + c_{22}^0 \frac{1}{r^2}\frac{\partial}{\partial \theta} + c_{66}^0 \left( \frac{1}{r}\frac{\partial^2}{\partial r \partial \theta} + \frac{1}{r^2}\frac{\partial}{\partial \theta} + \frac{\lambda_2}{a}\frac{1}{r}\frac{\partial}{\partial \theta} \right)$$

$$E_{22} = c_{22}^0 \frac{1}{r^2}\frac{\partial^2}{\partial \theta^2} + c_{44}^0 \left( \frac{\partial^2}{\partial z^2} + \frac{\lambda_1}{h}\frac{\partial}{\partial z} \right) + c_{66}^0 \left( \frac{1}{r}\frac{\partial}{\partial r} + \frac{\partial^2}{\partial r^2} - \frac{\lambda_2}{a}\frac{1}{r} + \frac{\lambda_2}{a}\frac{\partial}{\partial r} - \frac{1}{r^2} \right) - \rho^0 \frac{\partial^2}{\partial t^2}$$

$$E_{23} = c_{23}^0 \frac{1}{r}\frac{\partial^2}{\partial \theta \partial z} + c_{44}^0 \left( \frac{1}{r}\frac{\partial^2}{\partial \theta \partial z} + \frac{\lambda_1}{h}\frac{1}{r}\frac{\partial}{\partial \theta} \right)$$

$$E_{13} = c_{13}^0 \left( \frac{\partial^2}{\partial r \partial z} + \frac{\lambda_1}{h}\frac{\partial}{\partial r} \right) + c_{23}^0 \left( \frac{1}{r}\frac{\partial}{\partial z} + \frac{\lambda_1}{h}\frac{1}{r} \right) + c_{55}^0 \left( \frac{1}{r}\frac{\partial}{\partial z} + \frac{\partial^2}{\partial r \partial z} + \frac{\lambda_2}{a}\frac{\partial}{\partial z} \right)$$

$$E_{32} = c_{23}^0 \left( \frac{1}{r}\frac{\partial^2}{\partial \theta \partial z} + \frac{\lambda_1}{h}\frac{1}{r}\frac{\partial}{\partial \theta} \right) + c_{44}^0 \frac{1}{r}\frac{\partial^2}{\partial \theta \partial z}$$

$$E_{33} = c_{33}^0 \left( \frac{\partial^2}{\partial z^2} + \frac{\lambda_1}{h}\frac{\partial}{\partial z} \right) + c_{44}^0 \frac{1}{r^2}\frac{\partial^2}{\partial \theta^2} + c_{55}^0 \left( \frac{1}{r}\frac{\partial}{\partial r} + \frac{\partial^2}{\partial r^2} + \frac{\lambda_2}{a}\frac{\partial}{\partial r} \right) - \rho^0 \frac{\partial^2}{\partial t^2}$$

(A.1)

$$m_{11} = \frac{h^2}{a^2}\left[-\frac{\bar{c}_{11}^0}{\bar{c}_{55}^0}\left(\frac{1}{R}\frac{\partial}{\partial R} + \frac{\partial^2}{\partial R^2} + \lambda_2\frac{\partial}{\partial R}\right) - \frac{\bar{c}_{12}^0}{\bar{c}_{55}^0}\frac{\lambda_2}{R} + \frac{\bar{c}_{22}^0}{\bar{c}_{55}^0}\frac{1}{R^2} + \frac{\bar{c}_{66}^0}{\bar{c}_{55}^0}\frac{\beta_m^2}{R^2}\right] - \frac{\bar{c}_{11}^0}{\bar{c}_{55}^0}\Omega^2$$

$$m_{12} = \frac{\beta_m h^2}{Ra^2}\left[\frac{\bar{c}_{12}^0}{\bar{c}_{55}^0}\left(\frac{\partial}{\partial R} + \lambda_2\right) - \frac{\bar{c}_{22}^0}{\bar{c}_{55}^0}\frac{1}{R} + \frac{\bar{c}_{66}^0}{\bar{c}_{55}^0}\left(\frac{\partial}{\partial R} - \frac{1}{R}\right)\right]$$

$$m_{13} = -\frac{\lambda_1 h}{a}\frac{\partial}{\partial R}$$

$$m_{21} = -\frac{\beta_m h^2}{Ra^2}\left[\frac{\bar{c}_{12}^0}{\bar{c}_{44}^0}\left(\frac{\partial}{\partial R}\right) + \frac{\bar{c}_{22}^0}{\bar{c}_{44}^0}\frac{1}{R} + \frac{\bar{c}_{66}^0}{\bar{c}_{44}^0}\left(\frac{\partial}{\partial R} + \frac{1}{R} + \lambda_2\right)\right]$$

$$m_{22} = \frac{h^2}{a^2}\left[\frac{\bar{c}_{22}^0}{\bar{c}_{44}^0}\frac{\beta_m^2}{R^2} - \frac{\bar{c}_{66}^0}{\bar{c}_{44}^0}\left(\frac{1}{R}\frac{\partial}{\partial R} + \frac{\partial^2}{\partial R^2} - \frac{\lambda_2}{R} + \lambda_2\frac{\partial}{\partial R} - \frac{1}{R^2}\right)\right] - \frac{\bar{c}_{11}^0}{\bar{c}_{44}^0}\Omega^2$$

$$m_{23} = \frac{\lambda_1\beta_m h}{Ra}\quad,\quad m_{31} = -\frac{\lambda_1 h}{a}\left[\frac{\bar{c}_{13}^0}{\bar{c}_{33}^0}\frac{\partial}{\partial R} + \frac{\bar{c}_{23}^0}{\bar{c}_{33}^0}\frac{1}{R}\right] \tag{A.2}$$

$$m_{32} = \frac{\bar{c}_{23}^0}{\bar{c}_{33}^0}\frac{\lambda_1\beta_m h}{Ra}\quad,\quad m_{33} = \frac{h^2}{a^2}\left[\frac{\bar{c}_{44}^0}{\bar{c}_{33}^0}\frac{\beta_m^2}{R^2} - \frac{\bar{c}_{55}^0}{\bar{c}_{33}^0}\left(\frac{1}{R}\frac{\partial}{\partial R} + \frac{\partial^2}{\partial R^2} + \lambda_2\frac{\partial}{\partial r}\right)\right] - \frac{\bar{c}_{11}^0}{\bar{c}_{33}^0}\Omega^2$$

$$m'_{11} = -\lambda_1\quad,\quad m'_{12} = 0\quad,\quad m'_{13} = \frac{h}{a}\left[-\frac{\bar{c}_{13}^0}{\bar{c}_{55}^0}\left(\frac{\partial}{\partial R} + \frac{1}{R} + \lambda_2\right) + \frac{\bar{c}_{23}^0}{\bar{c}_{55}^0}\frac{1}{R}\frac{\partial}{\partial R}\right]$$

$$m'_{21} = 0\quad,\quad m'_{22} = -\lambda_1\quad,\quad m'_{23} = -\frac{\beta_m h}{Ra}\left(\frac{\bar{c}_{23}^0}{\bar{c}_{44}^0} + 1\right)$$

$$m'_{31} = -\frac{h}{a}\left[\frac{\bar{c}_{55}^0}{\bar{c}_{33}^0}\left(\frac{\partial}{\partial R} + \frac{1}{R} + \lambda_2\right) + \frac{\bar{c}_{23}^0}{\bar{c}_{33}^0}\frac{1}{R} + \frac{\bar{c}_{13}^0}{\bar{c}_{33}^0}\frac{\partial}{\partial R}\right]$$

$$m'_{32} = \frac{\beta_m h}{Ra}\left(\frac{\bar{c}_{23}^0}{\bar{c}_{33}^0} + \frac{\bar{c}_{44}^0}{\bar{c}_{33}^0}\right)\quad,\quad m'_{33} = -\lambda_1$$

## REFERENCES

[1]    Reddy J.N., Zhen-Qiang Ch., 2002, Frequency correspondence between membranes and functionally graded spherical shallow shells of polygonal plan form, *International Journal of Mechanical Sciences* **44**: 967-985.

[2]    Efraim E., Eisenberger M., 2007, Exact vibration analysis of variable thickness thick annular isotropic and FGM plates, *Journal of Sound and Vibration* **299**: 720-738.

[3]    Nie G.J., Zhong Z., 2007, Semi-analytical solution for three-dimensional vibration of functionally graded circular plates, *Computer Methods in Applied Mechanics and Engineering* **196**: 4901-4910.

[4]    Dong C.Y., 2008, Three-dimensional free vibration analysis of functionally graded annular plates using the Chebyshev–Ritz method, *Materials and Design* **29**: 1518-1525.

[5]    Malekzadeh P., Shahpari S.A., Ziaee H.R., 2010, Three-dimensional free vibration of thick functionally graded annular plates in thermal environment, *Journal of Sound and Vibration* **329**: 425-442.

[6]    Zahedinejad P., Malekzadeh P., Farid M., Karami G., 2010, A semi-analytical three dimensional free vibration analysis of functionally graded curved panels, *International Journal of Pressure Vessels and Piping* **87**: 470-480.

[7]    Zhao X., Liew K.M., 2011, Free vibration analysis of functionally graded conical shell panels by a meshless method, *Composite Structures* **93**: 649-664.

[8]    Nemat-Alla M., 2003, Reduction of thermal stresses by developing two dimensional functionally graded materials, *International Journal of Solids and Structures* **40**: 7339-7356.

[9]    Nie G., Zhong Zh., 2010, Dynamic analysis of multi-directional functionally graded annular plates, *Applied Mathematical Modelling* **34**: 608-616.

[10]   Su Zh., Jin G., Shi Sh., Ye T., Jia X., 2014, A unified solution for vibration analysis of functionally graded cylindrical, conical shells and annular plates with general boundary conditions, *International Journal of Mechanical Sciences* **80**: 62-80.

[11]     Zhang S.L., Zhang Z.X., Xin Z.X., Pal K., Kim J.K., 2010, Prediction of mechanical properties of polypropylene/waste ground rubber tire powder treated by bitumen composites via uniform design and artificial neural networks, *Materials & Design* **31**: 1900-1905.

[12]     Ashrafi H.R., Jalal M., Garmsiri K., 2010, Prediction of load–displacement curve of concrete reinforced by composite fibers (steel and polymeric) using artificial neural network, *Expert Systems with Applications* **37**(12): 7663-7668.

[13]     Anderson D., Hines E.L., Arthur S.J., Eiap E.L., 1997, Application of artificial neural networks to the prediction of minor axis steel connections, *Composite Structures* **63**: 685-692.

[14]     Arslan M.A., Hajela P., 1997, Counter propagation neural networks in decomposition based optimal design, *Composite Structures* **65**: 641-650.

[15]     Ootao Y., Tanigawa Y., Nakamura T., 1999, Optimization of material composition of FGM hollow circular cylinder under thermal loading, a neural network approach, *Composites Part B* **30**: 415-422.

[16]     Han X., Xu D., Liu G.R., 2003, A computational inverse technique for material characterization of a functionally graded cylinder using a progressive neural network, *Neuro Computing* **51**: 341-360.

[17]     Jodaei A., Jalal M., Yas M.H., 2012, Free vibration analysis of functionally graded annular plates by state-space based differential quadrature method and comparative modeling by ANN, *Composites Part B* **43**: 340-353.

[18]     Jodaei A., Jalal M., Yas M.H., 2013,Three-dimensional free vibration analysis of functionally graded piezoelectric annular plates via SSDQM and comparative modeling by ANN, *Mathematical and Computer Modelling* **57** (5–6): 1408-1425.

[19]     Chen W.Q., Lv C.F., Bian Z.G., 2003, Elasticity solution for free vibration of laminated beams, *Composite Structures* **62**: 75-82.

[20]     Shu C., Richards B.E., 1992, Application of generalized differential quadrature to solve two-dimensional incompressible Navier–Stokes equations, *International Journal for Numerical Methods in Fluids* **15**: 791-798.

[21]     Shu C., 2000, *Differential Quadrature and its Application in Engineering*, Berlin, Springer.

[22]     Bert C.W., Malik M., 1996, Differential quadrature method in computational mechanics, a review, *Applied Mechanics Reviews* **49**: 1-28.

[23]     Gantmacher F.R., 1960, *The Theory of Matrix*, Chelsea, New York.

[24]     Haykin S., 2000, *Neural Networks-A Comprehensive Foundation*, New York, Macmillan College Publishing Company.